

# N-Heterocyclic Organic Compounds as Additives For A-C Electrolytic Coloring of Anodized Aluminum From Nickel Sulfate Solutions Part II. Mechanism of Their Action

By B. Karagianni, I. Tsangaraki-Kaplanoglou

**In this study, an attempt was made to investigate the mechanism of the action of piperidine-4-carboxylic acid in comparison with piperidine-3-carboxylic acid during a-c electrolytic coloring of anodized aluminum in nickel sulfate-boric acid solution. Electrochemical impedance spectroscopy (EIS) data were used, as well as some other electrochemical techniques. Conformations of the additives that influence action between the opposite charges seem to play a significant role. They are correlated with the ability of the additive to be adsorbed on the electrode surface despite the alternating current, to interfere in the re-anodizing process, and in the nickel deposition rate and distribution.**

In Part I of our study,<sup>1</sup> several N-heterocyclic compounds were used as additives during the electrolytic coloring of anodized aluminum from nickel sulfate solutions. It was recognized that some of them improve the throwing power (TP) and/or the color intensity of the probes when added to the coloring baths in certain ranges of concentration. This effectiveness was correlated with their aromatic or saturated character, the position of their characteristic groups and the number of carbon atoms in their rings.

The best influence on the color intensity of the probes was observed in the case of piperidine-4-carboxylic acid, which also improves the TP. It is interesting, therefore, to study in more detail its mode of action and to compare it with that of piperidine-3-carboxylic acid, which has the same positive influence on TP, but not on color intensity. For this reason,

electrochemical impedance spectroscopy (EIS) has been used to characterize the surface of electrolytically colored anodized aluminum, during the earlier stages of the a-c coloring treatment, with the presence of the above additives at a higher voltage. EIS is a new technique in development and has been already used to elucidate the process of sealing<sup>2-4</sup> and to clarify a-c electrolytic coloring theoretically.<sup>5-7</sup> In this study, an attempt will be made to gain new information about the effect of these two additives on the anodized aluminum surface, and to elucidate their role during a-c electrolytic coloring in nickel sulfate baths.

Other instrumentation, such as the oscillograph, was also used in the present study for some electrical characteristics of the barrier layer to be measured. They were compared with those from EIS for the proposed mechanism, according to the EIS data,<sup>8,9</sup> to be confirmed.

## Experimental Procedure

Test specimens of 1050 aluminum alloy foil with dimensions 2 x 4 x 0.1 cm were used. The surface of the specimen was covered with araldite (epoxy resin), except for a unit area of 10.7 cm<sup>2</sup>. The samples were pre-treated, anodized, and electrolytically colored, as in Part I.<sup>1</sup> The electrolytic coloring baths contained:

The reference solution T (30 g/L NiSO<sub>4</sub> · 6H<sub>2</sub>O and 30 g/L H<sub>3</sub>BO<sub>3</sub>)

Solution A (solution T plus 0.07 g/L piperidine-4-carboxylic acid)

Solution B (solution T plus 0.07 g/L piperidine-3-carboxylic acid)

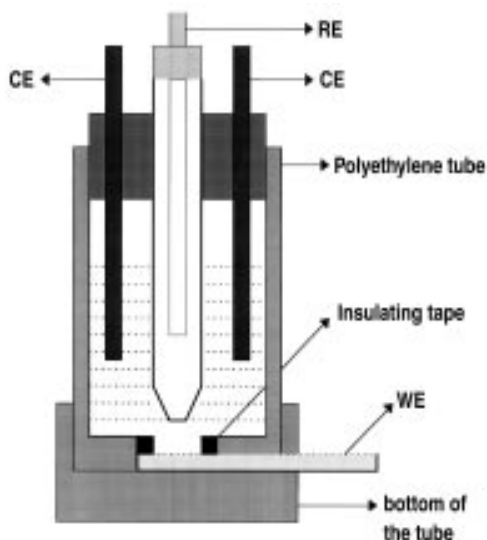


Fig. 1—Cross section of test cell. RE - Reference Electrode (SCE), CE - Counter-Electrode, WE - Working Electrode (specimen area 1.936 cm<sup>2</sup>).

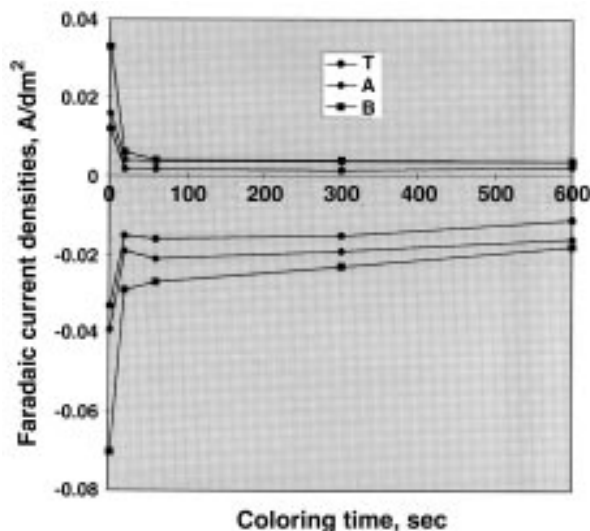


Fig. 2—Anodic and cathodic faradaic current densities at 1 and 20 sec, 1, 5 and 10 min of electrolytic coloring of anodized aluminum samples in solutions T, A and B.

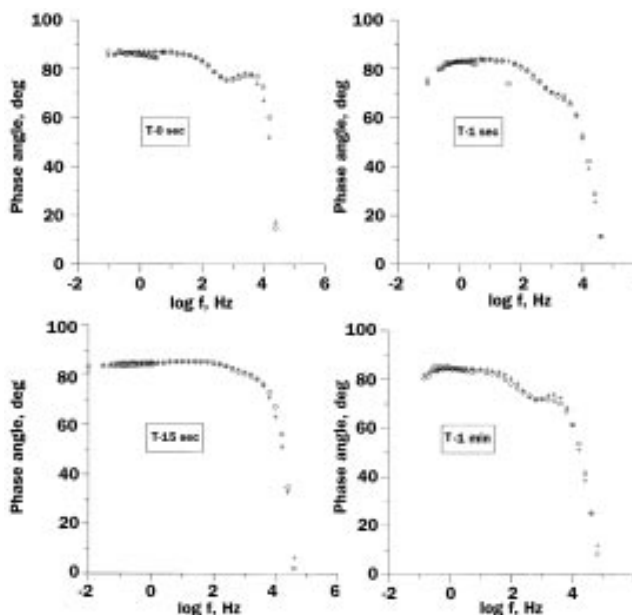


Fig. 3—Phase-angle Bode diagrams obtained in solution T for electrolytically colored aluminum probes for 0, 1, 15 sec and 1 min, (° measurement, + simulation).

## Measurements

### Oscillographic Measurements

A dual-channel digital storage oscilloscope was connected to a recorder to obtain voltage and current traces that were recorded at 1 sec, 20 sec, 1 min, 5 min and 10 min during electrolytic coloring.

### Impedance Measurements

A-C impedance measurements were carried out in solutions T, A and B at 25 °C and by using a cell such as that depicted in Fig. 1. Two short-circuited carbon rods served as the counter-electrodes (CE) and were placed across the two sides of the working electrode. A saturated calomel electrode (SCE) without Luggin capillary was used as the reference electrode.

A potentiostat with a lock-in amplifier, controlled by a personal computer, was used for the a-c impedance measurements.<sup>10</sup> Stability of the open circuit potential (OCP) was established after 60 min polarization at OCP. The amplitude of the a-c signal was 10 mV (SCE) and the data collected at frequency intervals of 4 points per decade for the range from 100 kHz to 30 mHz. The interface impedances at various frequencies were detected by measuring the amplitude and phase shift of a-c voltage and current. The impedance data were analyzed using software (Equivalent Circuit, version 4.5) for simulation of the equivalent circuit.

### Chronopotentiometric Measurements

Chronopotentiometric potential curves were obtained by the use of a constant current power supply and a V-t recorder with a sweep rate of 60 cm/min. A carbon plate was used as anode and an anodized aluminum probe as cathode.

### Linear Voltage Sweep Method

A voltage from 0-20 V was applied by a constant current/voltage power supply at the rate of 3 V/sec. It was controlled by a personal computer via an IEEE-488 general purpose interface.

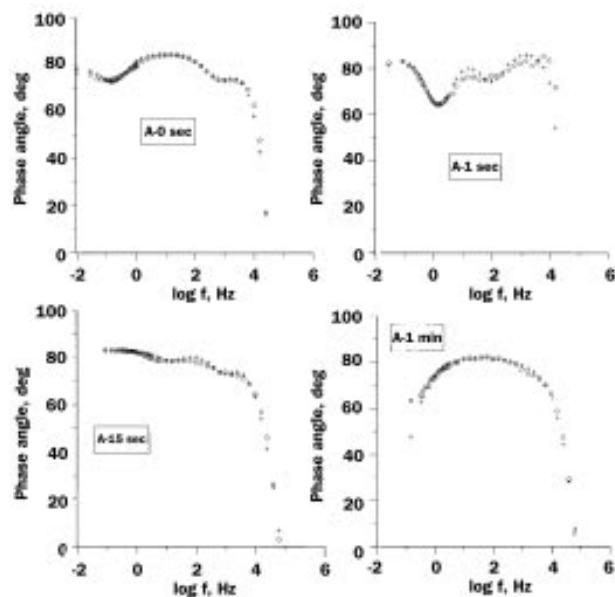


Fig. 4—Phase-angle Bode diagrams obtained in solution A for electrolytically colored aluminum probes for 0, 1, 15 sec and 1 min, (° measurement, + simulation).

## Energy Dispersive X-Ray Analysis

The anodized samples were electrolytically colored in the solutions T and A at 15 Vrms at 20 ± 1 °C for 5 and 15 sec, and 1, 2, 3, 5 and 10 min. The surface density of the deposited nickel on the probes was measured by energy dispersive X-ray fluorescence (XRF). The specimens were radiated with radioisotopes and the nickel X-rays produced were measured by a semiconductor detector.

## Results and Discussion

The anodic oxide layer that was formed on the aluminum surface at 18 VDC in 15-percent H<sub>2</sub>SO<sub>4</sub> (as referenced in the experimental section) consists of a very thin non-porous barrier layer and a thicker porous layer. The thickness of this barrier layer is reported to be about 18 nm.<sup>11</sup>

The a-c electrolytic coloring takes place at a cell voltage of 15 Vrms, which means about 21.2 V peak. Under these conditions, the barrier layer thickness increases during the earlier stages of this treatment to a large value governed by the peak voltage. This is the re-anodizing process.<sup>5,12</sup>

The presence of the semiconductive oxide layer causes a deformation of the sinusoidal current, which was observed on the oscillographs from the start of the a-c electrolytic coloring.<sup>12,13</sup> The deformed current waveform is divided into two parts, designated I<sub>Cp</sub> (capacitive current) and I<sub>F</sub> (faradaic or reaction current). A change of I<sub>Cp</sub> indicates a change of impedance in the electrolysis system and a change of I<sub>F</sub> indicates a change in the reaction rate.<sup>8</sup>

From Fig. 2 it is obvious that:

- The faradaic current densities decrease during the stage of re-anodizing (0-20 sec) until a value is reached that shows only a small additional decrease.
- The anodic reaction rates (I<sub>F</sub>) in solutions A and B are similar and higher than in T. This is attributed to a dissolution process of Al<sup>3+</sup> and is assumed to be related mainly to processes occurring at the barrier oxide/electrolyte interface.<sup>14</sup>
- The cathodic reaction rates (I<sub>F</sub>) are higher in the cases of solutions B and A. This is related in the former case to

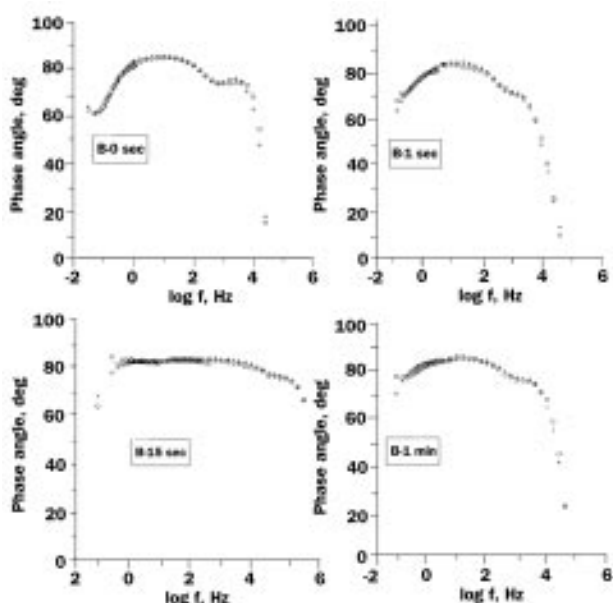


Fig. 5—Phase-angle Bode diagrams obtained in solution B for electrolytically colored aluminum probes for 0, 1, 15 sec and 1 min, (° measurement, + simulation).

greater hydrogen evolution, and in the latter case to greater nickel deposition, according to the coloring intensities data.<sup>1</sup>

Electrochemical impedance spectroscopy (EIS) is a method more suitable than the oscillograph measurements ( $I_{Cp}$ ) to characterize changes of impedance of the electrode. In this study, the more convenient mode for representation of the EIS data is the so-called phase-angle Bode plots of anodized aluminum samples. They permit examination of the phase shift ( $\delta$ ) (Figs. 3-5), as a function of frequency.

These data can be described by use of a parallel RC equivalent electric circuit.<sup>2-4,7</sup> The magnitude of the various contributing components of the barrier and porous layer, which describe their dielectric (capacitance, C) and electronic behavior (resistance, R) can also be extracted. The capacitance is unequivocally related to the thickness of the barrier oxide film, and the resistance corresponds to chemical processes occurring at the barrier oxide/electrolyte interface. The equivalent circuit of an aluminum oxide layer can be demonstrated by two parallel RC circuits connected in series, where the solution resistance  $R_s$  is added (Fig. 6).<sup>3</sup>

A third circuit appears, however, at the earlier stages of electrolytic coloring of anodized aluminum samples in the solutions A and B, as shown from the phase angle plots (Figs. 4-5). This third circuit demonstrates the presence of a modified barrier layer caused by the influence of the adsorbates A

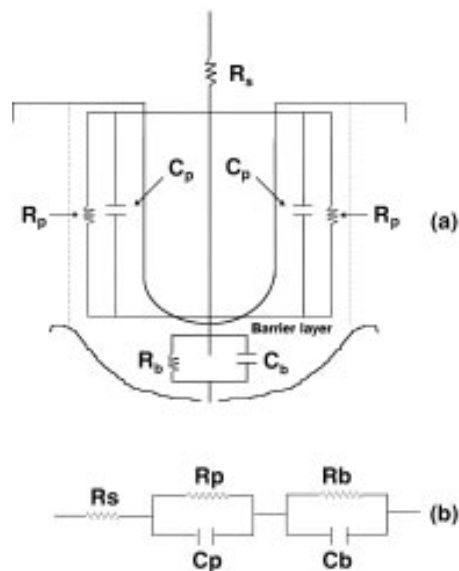


Fig. 6—Equivalent circuit models of anodized aluminum: (a) schematic diagram of porous anodic films; (b) equivalent electric circuit of (a) -  $R_s$ , electrolyte resistance;  $R_p$ , pore resistance;  $C_p$ , pore capacitance;  $R_b$ , barrier layer resistance;  $C_b$ , barrier layer capacitance.

and B (Fig. 7). Consequently, two barrier layers with different characteristics seem to exist. It is obvious from the table that the resistance of the modified barrier layer is much smaller than that of the normal layer.

Figures 8 and 9 show the capacitance of the normal and the modified barrier layers as functions of the duration of the electrolytic coloring. A completely different behavior of solutions T, A and B is observed during the first second of the coloring treatment. If it is considered that the dielectric constant of the barrier layer is not substantially differentiated, these values can be converted to thickness. Accordingly, the thicknesses (d) of the normal and of the modified barrier layers were calculated from the values of  $C_b$  and  $C_{bAD}$  by use of the following equation:<sup>3</sup>

$$C_b = \epsilon \cdot \epsilon_0 \cdot A/d,$$

where  $\epsilon_0$  is the permittivity of free space,  $8.85 \times 10^{-12}$  F/m,  $\epsilon$  is the dielectric constant of the film ( $\epsilon = 10$ ), and specimen area A is  $1.936 \times 10^{-4}$  m<sup>2</sup>.

The barrier layer thickness at the start of electrolytic coloring is much lower, 11 nm, than expected.<sup>11</sup> This probably means that there is an attack on the barrier layer, during the one-hr immersion in the slightly acidic solution, before the impedance measurements begin. A further decrease of barrier layer thickness is observed in the presence of additive A (3.6 nm) and that of B (5.6 nm). This can be explained by the assumption that this portion of the barrier layer was changed to another with modified electrical characteristics.

Because of the re-anodizing effect, the barrier layer thickness increases from 11 to 12 nm in the case of T during the first second of coloring treatment, while in the case of A, only the adsorbent barrier layer thickness increases from 3.6 to 10.5 nm, leading to a value [(6.8 + 10.5) nm] greater than that of T. This probably means promotion of re-anodizing. In the case of B, a sharp increase of barrier layer thickness from 5 to 10.2 nm is observed, while the thickness of the adsorbent barrier layer decreases from 5.6 to 2.3 nm and the total value is lower than T. After the one-sec treatment, a further increase

Resistance of the Barrier Layer ( $R_b$ ) and the Adsorbent Layer ( $R_{bAD}$ )  
Mohm-cm<sup>2</sup>

t sec	$R_b$ T	$R_b$ A	$R_b$ B	$R_{bAD}$ A	$R_{bAD}$ B
0	47.61	68.05	35.29	0.178	0.586
1	7.92	24.02	2.08	0.048	0.029
5	29.37	1.22	6.04	0.021	—
15	370.23	348.92	501.78	0.003	0.047
60	28.65	2.23	7.95	—	—

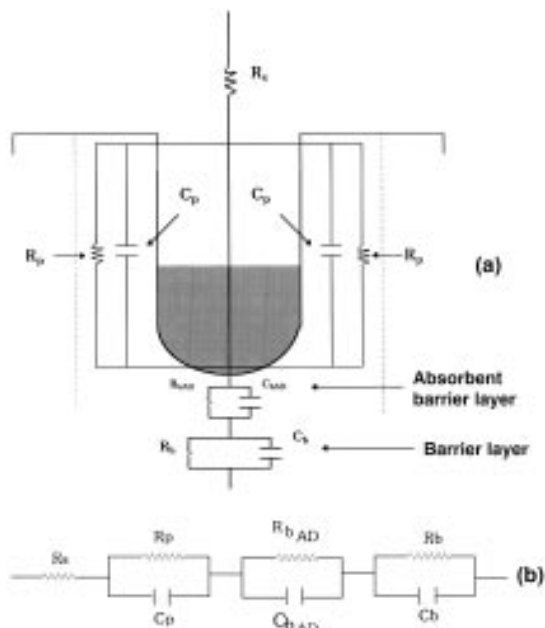


Fig. 7—Simplified equivalent circuit models of electrolytically colored anodized aluminum with a modified barrier layer: (a) schematic diagram; (b) equivalent electric circuit of (a) -  $R_{bAD}$  adsorbent barrier layer resistance;  $C_{bAD}$  adsorbent barrier layer capacitance.

of the barrier layer thickness is observed until the re-anodizing ceases. Finally, the adsorbent barrier layer thickness has an almost constant value (4-5 nm) in the case of A, until the time when re-anodizing ceases, while in the case of B, it decreases quickly from the commencement of electrolytic coloring. In this case, however, the total barrier layer thickness is lower than T, allowing a greater current to pass.

From Fig. 10, it is apparent that the amount of deposited nickel on the probes increases almost linearly for the first 5 min of treatment. Accordingly, the deposition rate can be expressed by the value of the one-degree polynomials to which the curves of Fig. 10 are fitted. These values are: 0.20 for solution T and 0.24 for A. This means that additive A increases the value of a and, consequently, the deposition rate from 0.20 to 0.24. From Fig. 10, it is also obvious that nickel deposition ceases later in the presence of additive A.

The cathodic polarization of the anodic oxide film in coloring baths T, A and B (Fig. 11), gives more information about the situation of the barrier layer as a function of the time of treatment under constant current density. An initial vertical increase of cathodic potential is observed that is related to the thickness of the barrier layer, according to Sato.<sup>9</sup> It is obvious from Fig. 11 that this potential is lower in the case of A, which implies a thinner barrier layer. As the oxide film continues to be cathodically polarized, the pH of the colloidal sol layer of aluminum hydroxide, which exists at the bottom of the pores of this film, rises to the pH of gelation of aluminum hydroxide.<sup>9</sup> Then the sol layer changes into a gel layer. This gel layer is the cause of the second rise in cathodic potential.<sup>9</sup> This increase is lower in the case of A than for T (Fig. 11), and more time is needed for the final value to be reached. This means that the process of gelation takes place at a lower rate and extent in the case of A than for T during cathodic polarization, and that only a portion of the barrier layer is transformed to a gel.

The thinner barrier layer in the case of A, which means a lower extent of gelation, is also confirmed by the curves of Fig. 12, where the cathodic current peak appears at a lower

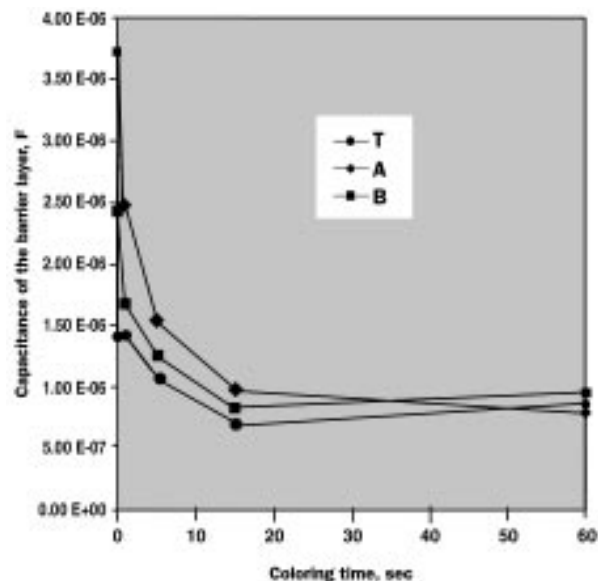


Fig. 8—Capacitance of the barrier layer of anodized aluminum as a function of coloring time in solutions T, A and B.

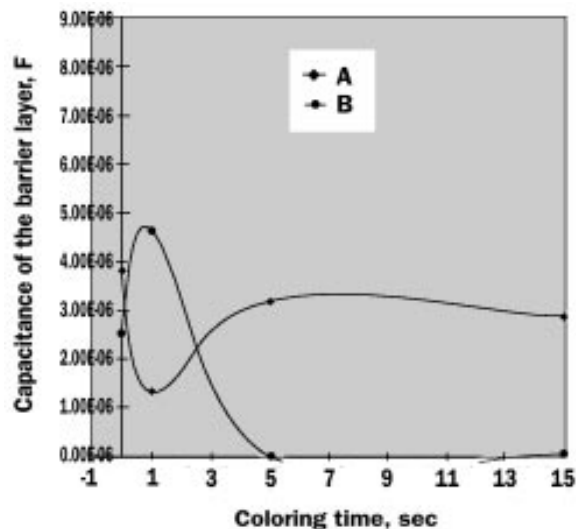


Fig. 9—Capacitance of the adsorbent barrier layer of anodized aluminum as a function of coloring time in solutions A and B.

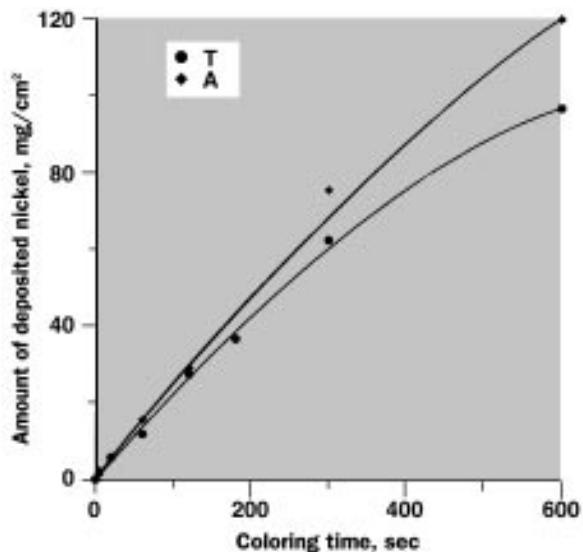


Fig. 10—Nickel content of electrolytically colored aluminum probes in solutions T and A as a function of coloring time.

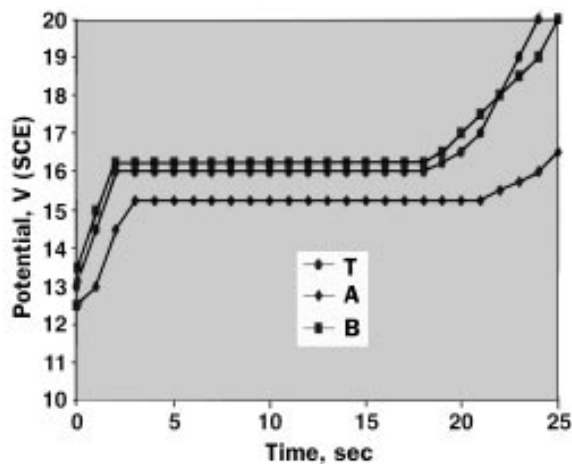


Fig. 11—Cathodic potential change of anodic oxide film as a function of time in solutions T, A and B.

voltage,<sup>8</sup> and the first small peak is lower than in the cases of T and B. In this latter case, B, more gelation seems to occur and accordingly, a somewhat higher potential than that of T is observed.

#### Conclusions

The re-anodizing process which takes place during electrolytic coloring appears to be influenced by the presence of 3- and 4- piperidinecarboxylic acids in a different way, especially during the first second. When piperidine-4-carboxylic acid is present, a thicker barrier layer, as a whole, is produced during the first second of coloring, although the electrical characteristics of a portion of it are modified. This is likely because piperidine-4-carboxylic acid retards the process of gelation of aluminum hydroxide during the cathodic half-cycle. This seems also to contribute to the increase of the nickel deposition rate. This behavior is determined by its stereochemical conformations. The six-membered saturated N-heterocyclics prefer the chair conformation in which the equatorial orientation of the carboxyl group is dominant.<sup>15</sup> In our case, however, the piperidine-4-carboxylic acid continues to be adsorbed on the aluminum oxide despite the applied alternating electric field. This can be explained by the assumption that the boat conformation of this additive predominates (Fig. 13). This brings the opposite charges of the molecule within a critical distance, which permits interactions with the corresponding positive/negative sites of the substrate momentarily positioned close together, making

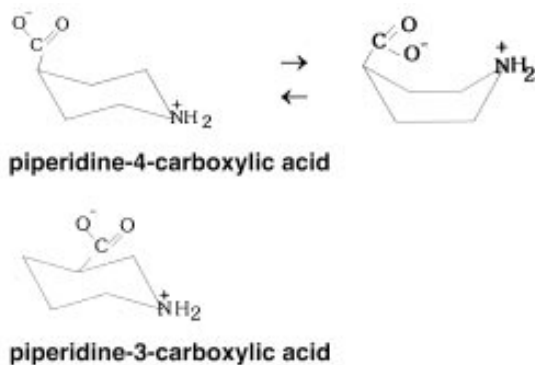


Fig. 13—Proposed conformations of the additives 4- and 3-piperidinecarboxylic acids.

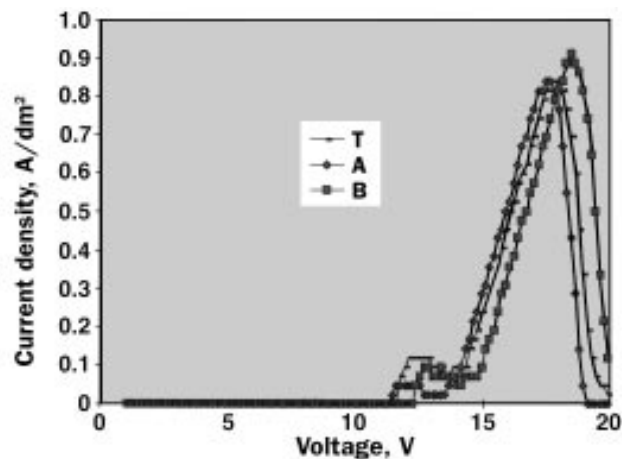


Fig. 12. Potentiodynamic curves for electrodeposition of nickel on anodic oxide films from solutions T, A and B at 3 V/sec sweep rate.

easier its adsorption on the electrode surface, not only at zero charge, but at positive and negative potentials as well.

By contrast, the piperidine-3-carboxylic acid is practically desorbed from the aluminum oxide when the alternating electric field is applied. This can be explained by the fact that the proper distance of the opposite charges of the molecule is not stereochemically permitted (Fig. 13); this is possible from the chair conformation with an axial carboxyl group, which, however, is not thermodynamically stable.

**Editor's note:** Manuscript received, October 1995; revision received, July 1996.

#### Acknowledgments

The authors wish to thank Dr. L. Kobotiatis (Centre of Applications and Technology of the Hellenic Air Force), assistant professor N. Kallithrakas and Dr. R. Moshohoritou (Lab. of Analyt. and Environmental Chemistry, Technical University of Crete) for their valued assistance.

#### References

1. B. Karagianni and I. Tsangaraki-Kaplanoglou, Part I of this study, *Plat. and Surf. Fin.*, **83**, 73 (Sept. 1996).
2. W. Paatsch, *J. Electrochem. Soc.*, **133**, 887 (1986).
3. M. Ahmadun, J. Dawson and G. Thompson, *Trans. Inst. Met. Fin.*, **68**, 109 (1990).
4. J. González, E. Ramirez, V. López and S. Flores, *Plat. and Surf. Fin.*, **82**, 54 (Oct., 1994).
5. K. Tachihara, Y. Itoi and E. Sato, *Electrochimica Acta*, **26**, 1299, (1981).
6. Y. Itoi *et al.*, *Electrochimica Acta*, **25**, 1297 (1980).
7. J. Cann, *J. Electrochem. Soc.*, **129**, 551 (1982).
8. T. Sato and S. Sakai, *Trans. Inst. Met. Fin.*, **57**, 43 (1979).
9. T. Sato, *Plat. and Surf. Fin.*, **78**, 70 (March 1991).
10. L. Kobotiatis, C. Tsirikas and P. Koutsoukos, *Corrosion*, **51**, 19 (Jan. 1995).
11. S. Wernick, R. Pinner and P.G. Sheasby, *The Surface Treatment of Aluminium and Its Alloys*, Vol. 1, ASM International, Metals Park, OH; Publications Ltd., Teddington, UK, 1987; p. 311.
12. N. Thorne, G. Thompson, R. Furneaux and G. Wood, *Proc. Symp. on Aluminum Surf. Treat. Technol.*, R.S. Alwitt and G.E. Thompson, eds., The Electrochemical Society, Pennington, NJ, 274 (1986).
13. B. Baker, *ibid.* 78 (1986).

14. D. Arrowsmith, D. Moth and A. Maddison, *Trans. Inst. Met. Fin.*, **65**, 38 (1987).
15. J. March, *Advanced Organic Chemistry, Reactions, Mechanisms and Structure*, 4th Ed., Wiley-Interscience, New York, NY, 1992; p. 147.

#### About the Authors



*Basiliki Karagianni is a doctoral candidate at the Laboratory of Industrial Chemistry, Dept. of Chemistry, University of Athens, Panepistimiopolis-Zografou, Athens 15771, Greece. Her research is in electrolytic coloring of anodized aluminum and improvement of the methods.*



*Dr. Irina Tsangaraki-Kaplanoglou is an associate professor at the University of Athens, Dept. of Chemistry, Laboratory of Industrial Chemistry. She has conducted research into the dyeing of aluminum by various processes and has collaborated in the work of the anodizing/anodic processes group of the Corrosion and Protection Centre at the University of Manchester Institute of Science and Technology. She holds a PhD from the University of Athens.*

---

#### AESF Offers 3 Classes

For Finishers in November:

Boston & Baltimore Inner Harbor

- 1. Training Course in Electroplating & Surface Finishing For Electronics Applications**  
November 11-14  
Days Inn Soldiers Field Rd., Boston, MA  
ESC or CEF-Se Exam, November 15  
Registration Deadline: October 30
- 2. Introduction to Electroplating & Surface Finishing**  
November 14-15  
Holiday Inn Baltimore Inner Harbor  
Registration Deadline: October 30
- 3. Training Course in Electroplating & Surface Finishing**  
November 18-21  
Holiday Inn Baltimore Inner Harbor  
CEF Exam, Nov. 22  
Registration Deadline: October 30



**To register or get more information, contact AESF's Educational Services Department.**

Phone: 407/281-6441

FAX: 407/281-6446

e-mail:

72420.2001@compuserve.com